

A simple and sensitive graphene oxide/nanogold SPR Rayleigh scattering-energy transfer analytical platform for detection of iodide and H₂O₂

Yaohui Wang, Xinghui Zhang, Qingye Liu, Guiqing Wen, Aihui Liang*, Zhiliang Jiang*

(Key Laboratory of Ecology of Rare and Endangered Species and Environmental Protection of Ministry Education, Guangxi Key Laboratory of Environmental Pollution Control Theory and Technology, Guangxi Normal University, Guilin 541004, China.)

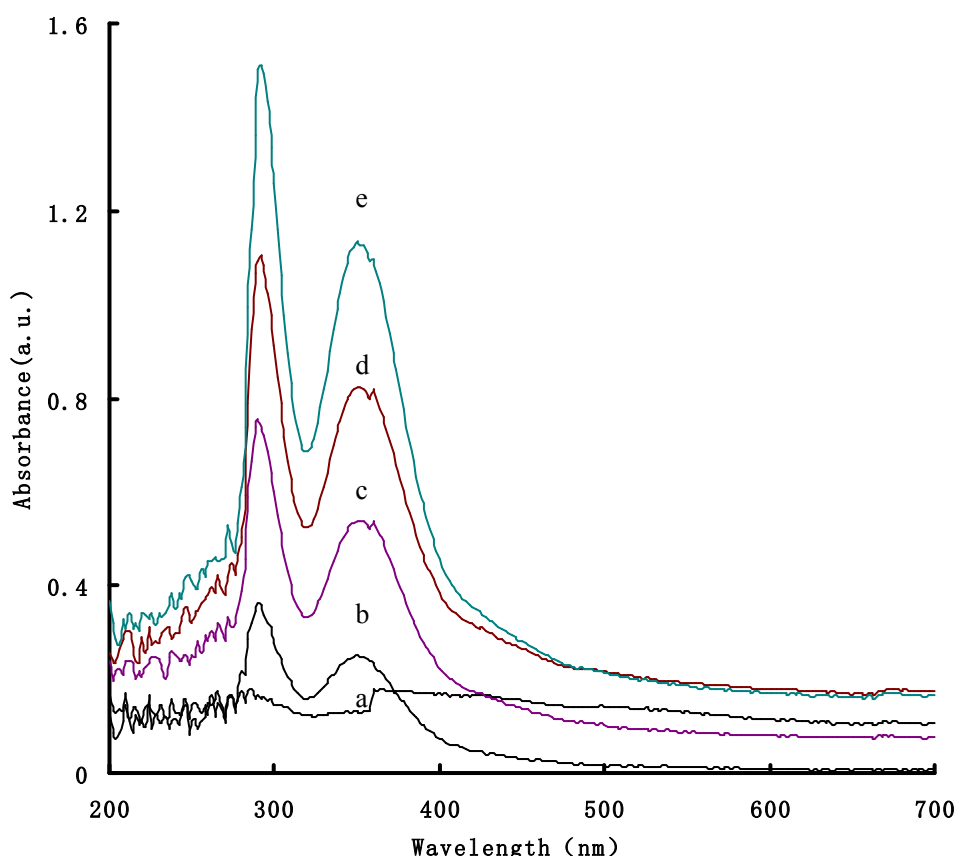


Fig. 1S Absorption spectra of the GO/GN-KI-KIO₃ system
(a) pH 2.8 Na₂HPO₄-citric acid-4mmol/LKI-4.78μg/mL GO/GN; (b) a+5μmol/L KIO₃; (c) a+10μmol/L KIO₃; (d) a+20μmol/L KIO₃; (e) a+25 μmol/L KIO₃.

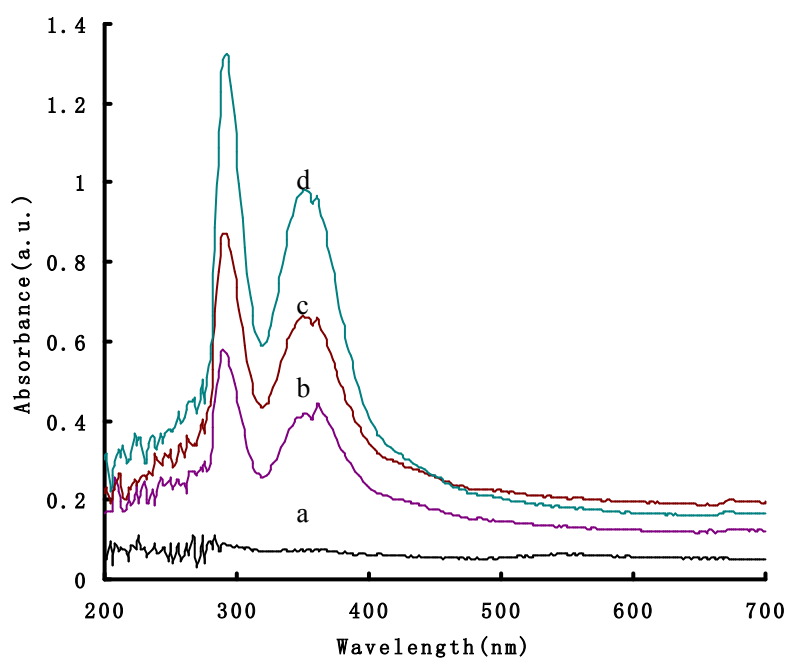


Fig. 2S Absorption spectra of the GN-KI-KIO₃ system

- (a) pH 2.8 Na₂HPO₄- citric acid-4mmol/L KI-4.782μg/ml GN; (b) a+15μmol/L KIO₃;
- (c) a+20μmol/L KIO₃; (d) a+25μmol/L KIO₃.

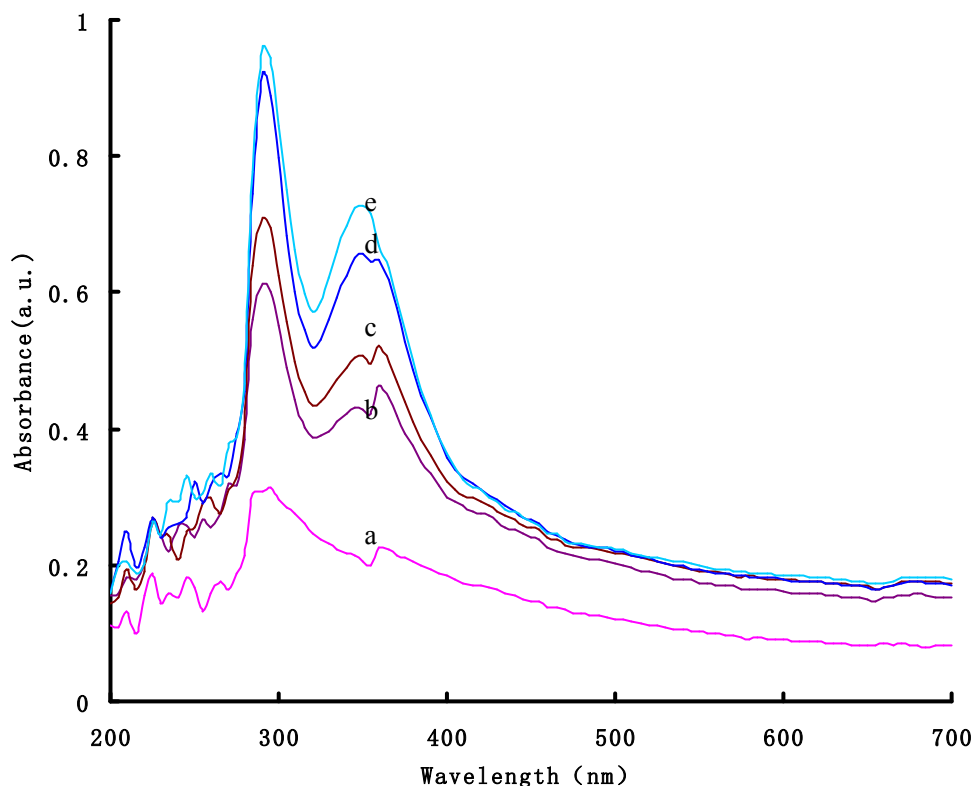


Fig. 3S Absorption spectra of the GO-KI-KIO₃ system

(a)pH 2.8 Na₂HPO₄-citric acid-4mmol/L KI-15μg/L GO; (b) a+5.5μmol/L KIO₃; (c)a+7μmol/L KIO₃; (d)a+8.5μmol/L KIO₃; (e)a+10μmol/L KIO₃.

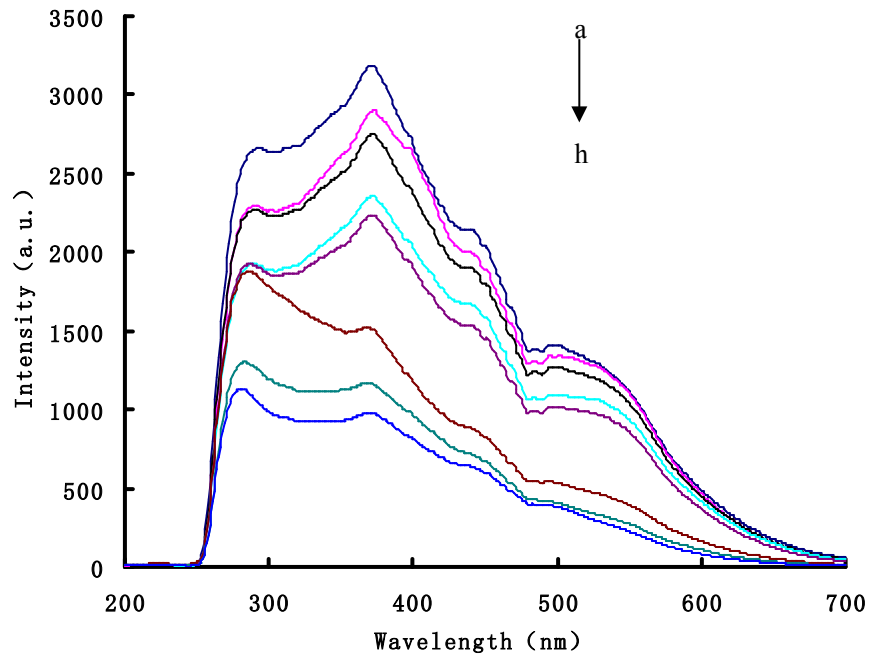


Fig. 4S RRS spectra of the GN-KI-KIO₃ system

(a) pH 2.8 Na₂HPO₄- citric acid-4mmol/L KI-4.782μg/ml GN; (b)a+0.25μmol/L KIO₃;(c) a+1μmol/L KIO₃; (d) a+2μmol/L KIO₃; (e) a+2.5μmol/L KIO₃;(f) a+4μmol/L KIO₃; (g) a+4.5μmol/L KIO₃; (h) a+5μmol/L KIO₃.

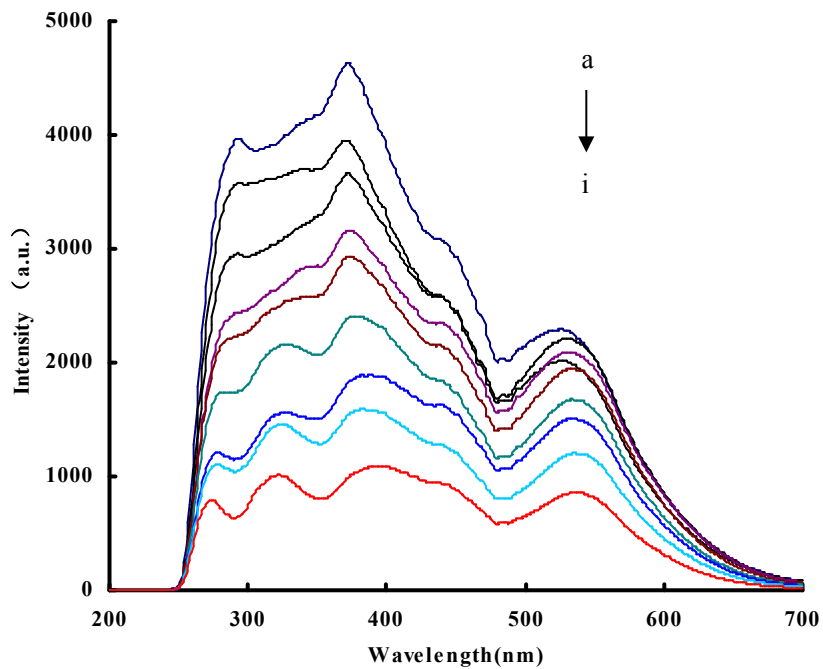


Fig. 5S RRS of the GN-KI-H₂O₂ system

(a) pH 3.4 Na₂HPO₄-citric acid-3mmol/L KI-4.782μg/ml GN; (b)a+10μmol/L H₂O₂; (c) a+20μmol/L H₂O₂; (d) a+30μmol/L H₂O₂; (e) a+40μmol/L H₂O₂; (f) a+50μmol/L H₂O₂; (g) a+60μmol/L H₂O₂; (h)a+70μmol/L H₂O₂; (i)a+80μmol/L H₂O₂

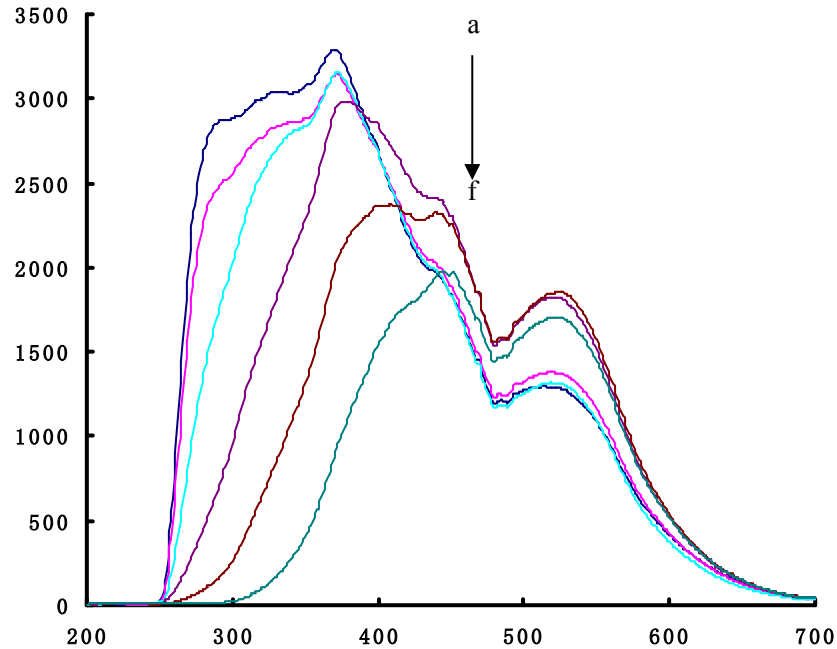


Fig. 6S RRS of the GN-KI-H₂O₂-Fe³⁺ catalytic system

(a) pH 2.8 Na₂HPO₄- citric acid-4mmol/L KI-25mmol/L H₂O₂-Fe³⁺-4.782μg/ml GN; (b) a+0.025mmol/L Fe³⁺; (c) a+0.1mmol/L Fe³⁺; (d) a+0.25mmol/L Fe³⁺; (e) a+0.5mmol/L Fe³⁺; (f) a+1mmol/L Fe³⁺.

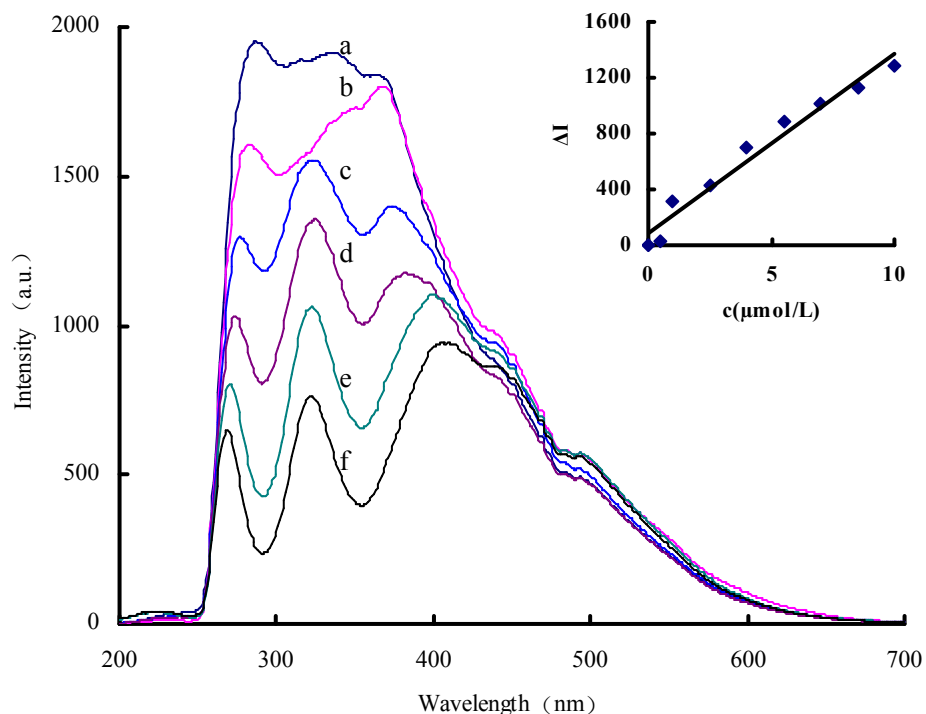


Fig. 7S RRS spectra of the GO-KI-KIO₃ system

(a) pH 2.8 Na₂HPO₄-citric acid-4mmol/L KI-15μg/L GO; (b)a+0. 5μmol/L KIO₃; (c) a+1μmol/L KIO₃; (d) a+2.5μmol/L KIO₃; (e) a+7μmol/L KIO₃; (f) a+10μmol/L KIO₃.

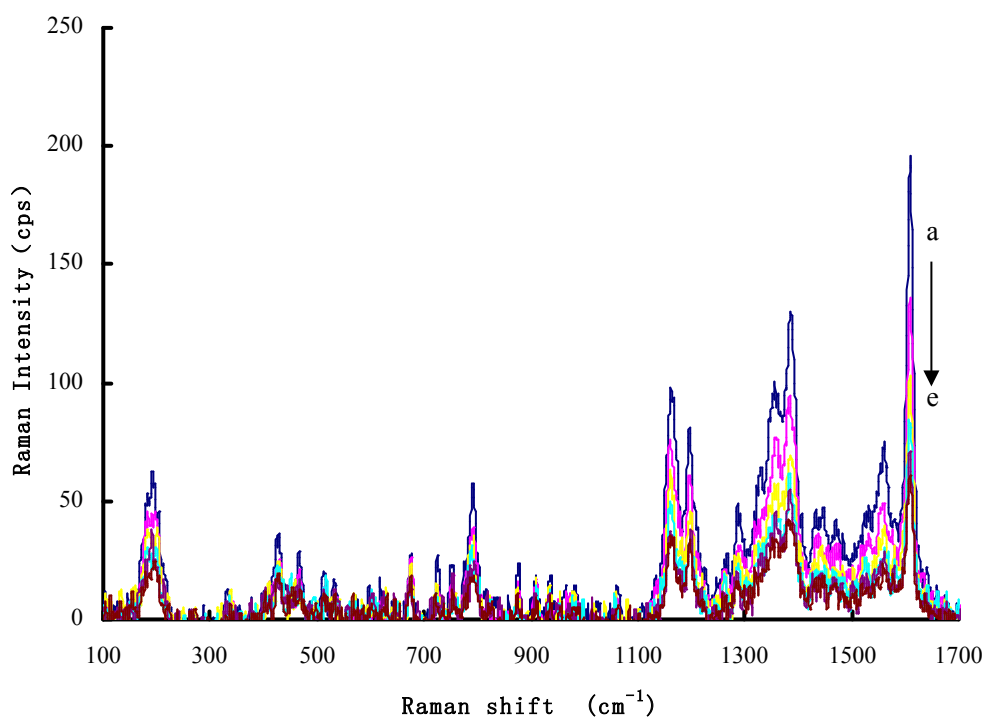


Fig. 8SA SERS spectra of KIO₃-KI-GN system

a: pH 2.8Na₂HPO₄-citric acid-4mmol/L KI-1.0μmol/L VBB-12μg/mL GN; b:

a+1 μ mol/L KIO₃; c: a+2.0 μ mol/L KIO₃; d: a+3.0 μ mol/L KIO₃; e: a+4.0 μ mol/L KIO₃.

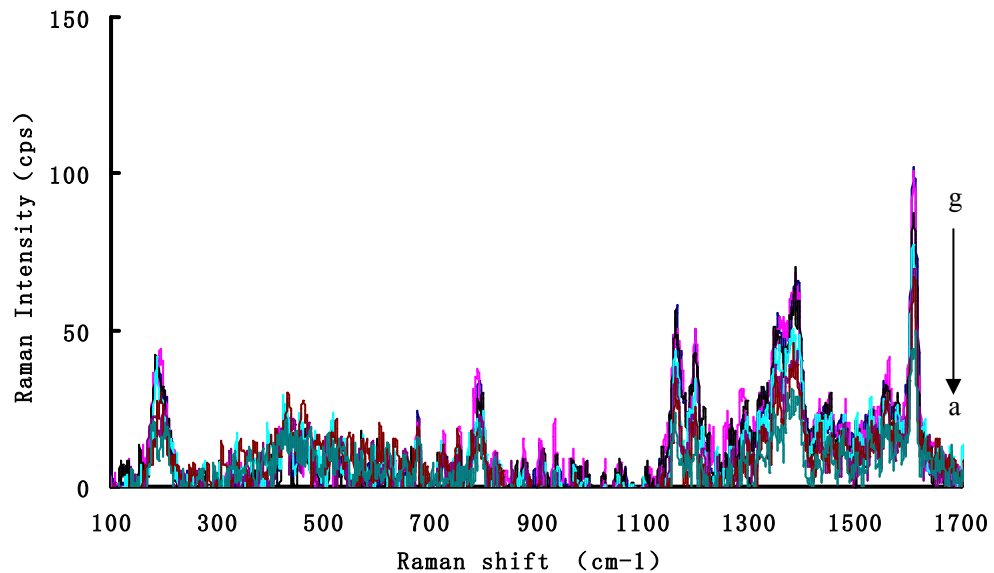
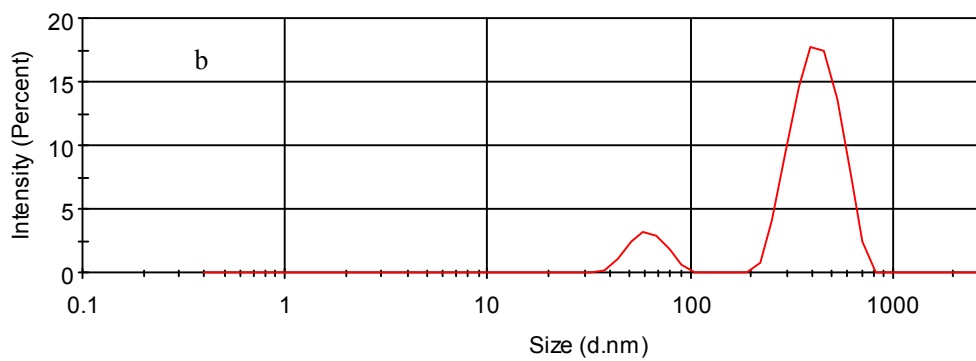
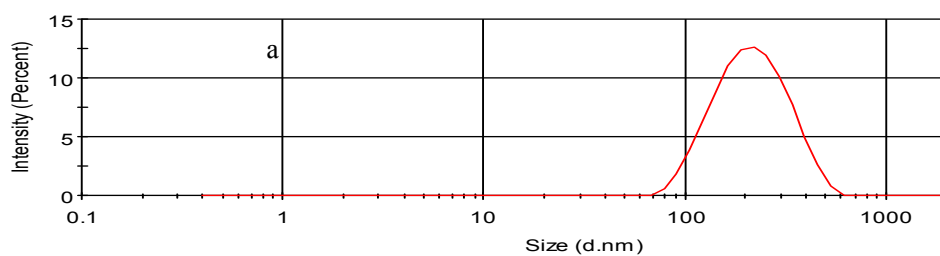


Fig. 8SB SERS spectra of KIO₃-KI-GO/GN system

a: pH 2.8Na₂HPO₄-citric acid-4mmol/L KI-1.0 μ mol/L VBB-12 μ g/mL GO/GN; b:
a+0.25 μ mol/L KIO₃; c: a+0.5 μ mol/L KIO₃; d: a+1 μ mol/L KIO₃; e: a+2.5 μ mol/L KIO₃;
f: a+4.0 μ mol/L KIO₃; g: a+5.5 μ mol/L KIO₃.



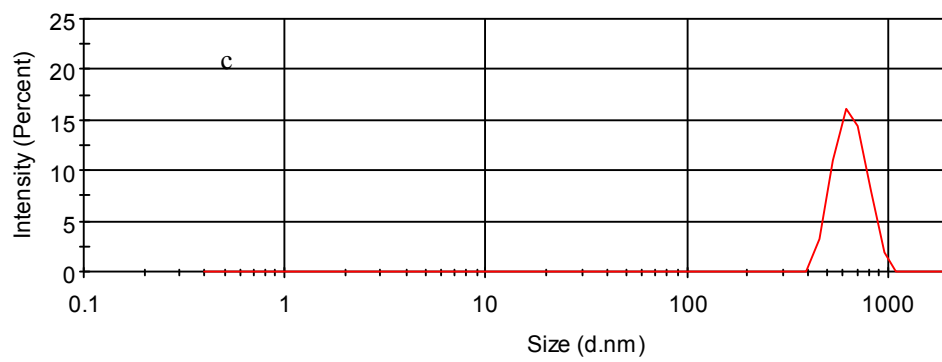


Figure 9S Laser scattering graph of the NG/GO systems

a: GO; b: GO/GN; c: GO/GN-2.8 Na₂HPO₄-citric acid-4 mmol/L KI-2.5 μmol/L KIO₃.

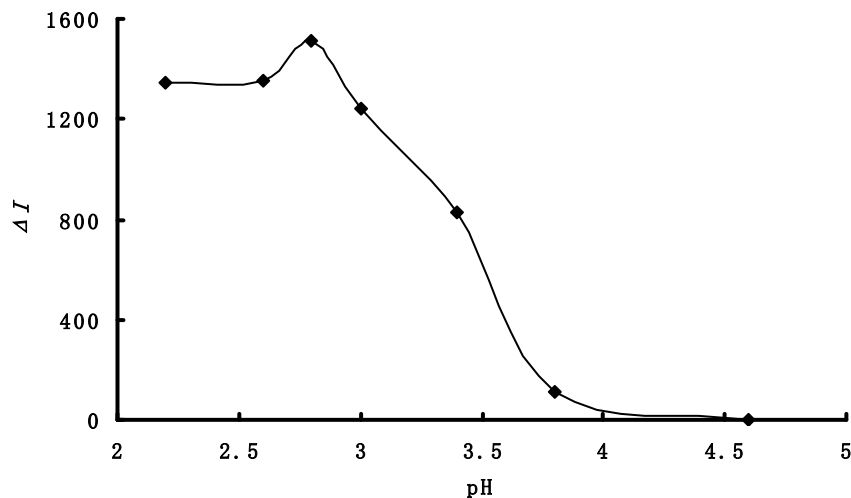


Fig. 10S Effect of pH Na₂HPO₄-citric acid buffer

3 mmol/L KI-2.5 μmol/L KIO₃-7.17 μg/mL GN

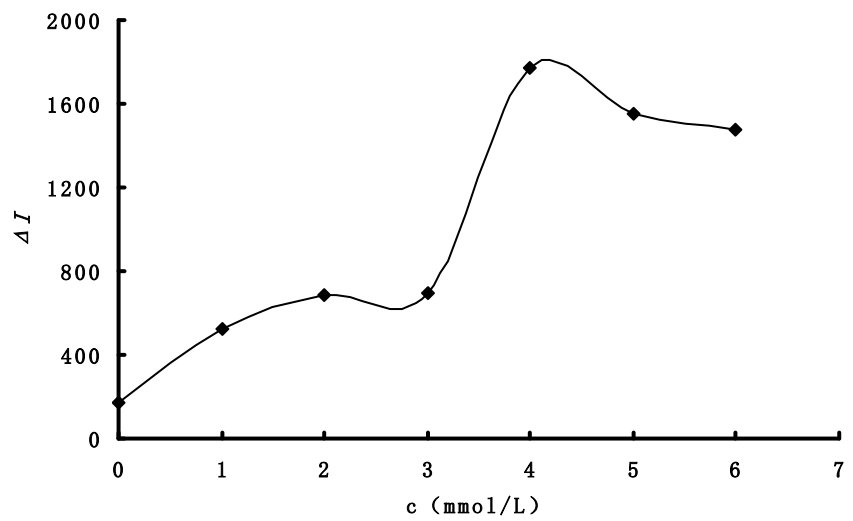


Fig. 11S Effect of KI concentration

pH 2.8Na₂HPO₄-citric acid buffer-2.5μmol/L KIO₃-7.173μg/mL GN

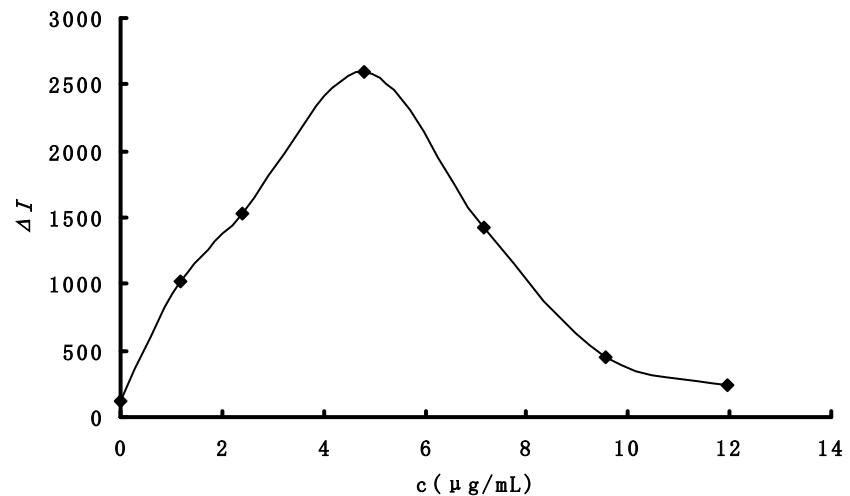


Fig. 12S Effect of GN concentration

pH 2.8Na₂HPO₄-citric acid buffer-4mmol/L KI-2.5μmol/L KIO₃

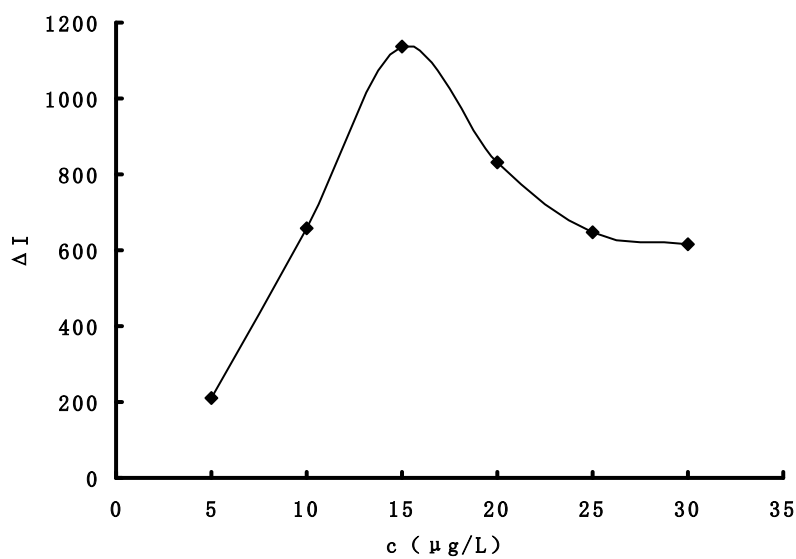


Fig. 13S Effect of GO concentration

pH 2.8Na₂HPO₄-citric acid buffer-4mmol/L KI-2.5 $\mu\text{mol/L}$ KIO₃.

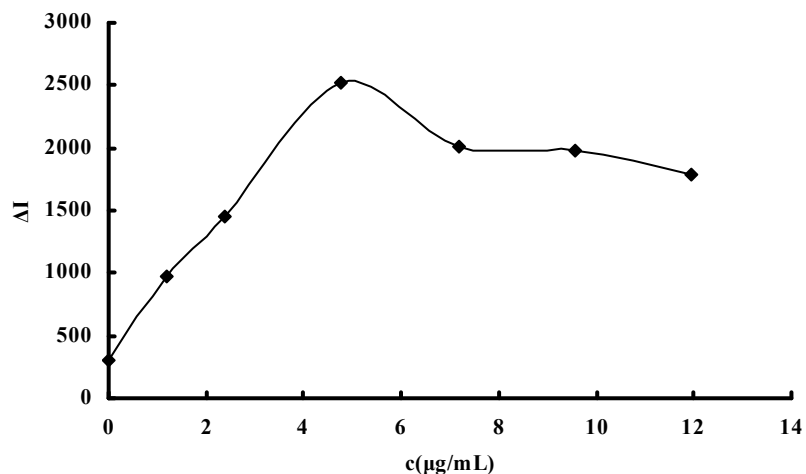


Fig. 14S Effect of GO/GN concentration

pH 2.8Na₂HPO₄-citric acid buffer-4mmol/L KI-2.5 $\mu\text{mol/L}$ KIO₃

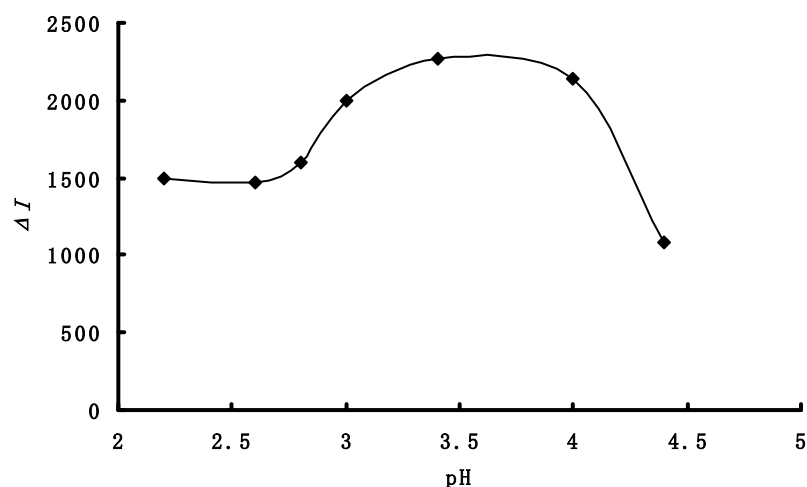


Fig. 15S Effect of pH Na₂HPO₄-citric acid buffer
3mmol/L KI-50μmol/L H₂O₂-7.173 μg/mL GN-50mmol/L NaCl

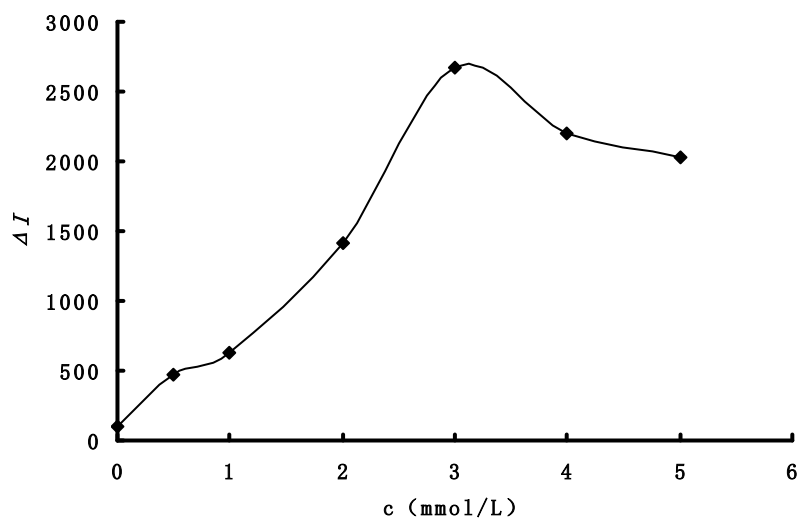


Fig. 16S Effect of KI concentration
pH3.4Na₂HPO₄-citric acid buffer-KI-50μmol/L H₂O₂-7.173μg/mL GN-50mmol/L
NaCl

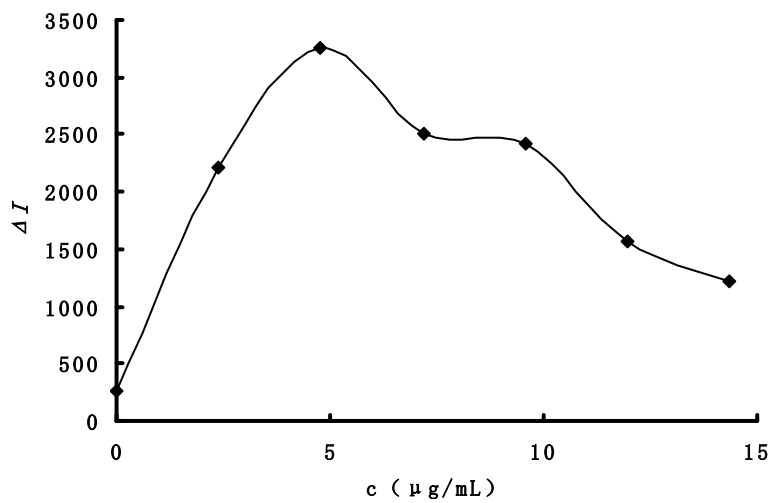


Fig. 17S Effect of GN concentration

pH 3.4Na₂HPO₄-citric acid buffer-3 mmol/L KI-50 $\mu\text{mol}/\text{L}$ H₂O₂- GN-50mmol/L NaCl

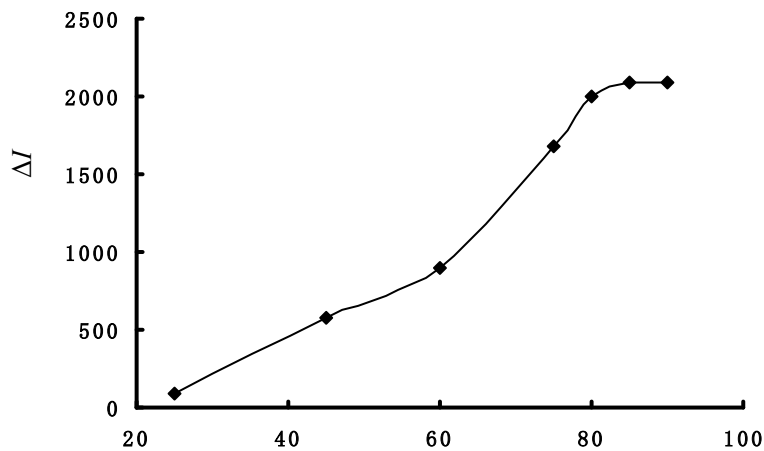


Fig. 18S Effect of temperature

pH 3.4Na₂HPO₄-citric acid-3 mmol/L KI-50 $\mu\text{mol}/\text{L}$ H₂O₂-4.782 $\mu\text{g}/\text{mL}$ GN.

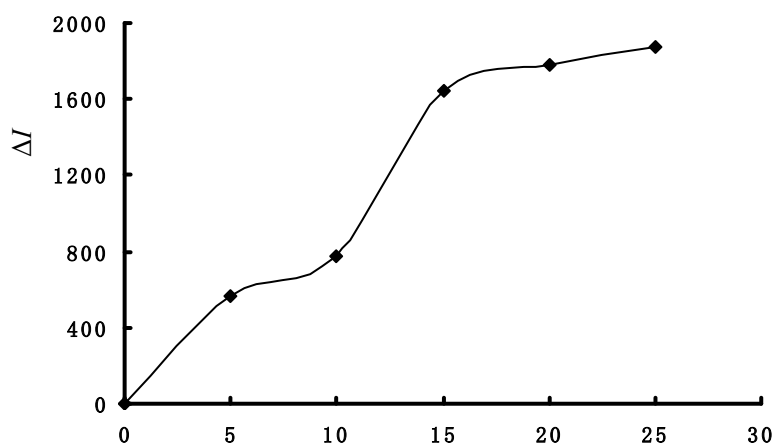


Fig. 19S Effect of reaction timepH 3.4 Na₂HPO₄-citric acid-3 mmol/L KI-50μmol/L H₂O₂-4.782μg/mL GN.**Table 1S** The reproducibility for some nanoparticle systems

System	Single value I	Average	RSD (%)
4.78μg/ml GN	197,210,235,201,1 94	207	8.0
pH 2.8 Na ₂ HPO ₄ -citric acid-4mmol/L KI-4365,3918,3537,33 4.78μg/ml GN	43,3803	3793	10.3
15μg/L GO	810,887,875,800,8 23	839	4.7
pH 2.8 Na ₂ HPO ₄ -citric acid-4mmol/L KI- 906,900,872,917,8 15μg/L GO	69	893	2.4
4.78μg/mL GO/GN	1394,1425,1282,13 51,1492	1389	5.7
pH 2.8 Na ₂ HPO ₄ -citric acid-4mmol/LKI- 1578,1727,1742,16 4.78μg/mL GO/GN	07,1558	1642	5.2

Table 2S Comparison of the reported methods for I

Method	Principle	LR (μmol/L)	DL (μmol/L)	Comments	Ref.
SM *	Iodate reacts with iodide to form I ₃ ⁻ that combined with starch to form blue complex with an absorption peak at 580 nm.	1.6-7.0	0.8	Simple, but low sensitivity	37
ISE	Using standard addition method and iodine ISE, iodine ion in iodine fortified beverages were determined.	0.5- 1.0×10 ⁵	0.63	Simple and automatic, but low sensitivity	38
IC-ICP/MS	Alkaline extraction and IC-ICP/MS were applied as the sample pretreatment method and the detection technique respectively, for iodate and iodide determination.	0.002-7.9	0.0008	Highly sensitive, but high-cost and complex.	39
Sensor	The colorimetric iodide sensor was based on the anti-aggregation of GNs that relied upon the distance-dependent optical properties of GNs, the combination of mercapto-functionalized thymine on GNs, and the stronger affinity between I ⁻ and Hg ²⁺ .	0.02-0.6	0.01	Simple and sensitive, but Hg ²⁺ used and complex.	33
RRS	Iodate reacts with iodide to form I ₃ ⁻ that combined with rhodamine 6G to form ion-associated particles with a RRS peak at 400 nm.	0.1-2.0	0.03	Simple, but low sensitivity	35

RRS-ET	The SPRRS energy of GO/GNs transferred to I_3^- complex that the decreased RRS intensity is linear to IO_3^- concentration.	0.025-5	0.008	Simple, fast, highly sensitive.	This paper
--------	---	---------	-------	---------------------------------------	---------------

* SM-spectrophotometric method, ISE-ion selective electrode, IC-ICP/MS-ion chromatography-inductively coupled plasma mass spectrometry.

Table 3S Effect of foreign substances on the determination of iodide

Coexistent substance	Tolerance Concentratio n ($\mu\text{mol/L}$)	Relative error (%)	Coexistent substance	Tolerance Concentratio n ($\mu\text{mol/L}$)	Relative error (%)
K ⁺	250	8.7	Ni ²⁺	250	3.0
Ca ²⁺	250	3.0	MoO ₄ ²⁻	200	-0.9
Zn ²⁺	250	2.4	SO ₄ ²⁻	250	-4.9
Glucose	200	-6.1	BrO ₃ ⁻	250	-2.0
Co ²⁺	250	-5.4	Cu ²⁺	200	0.8
Al ³⁺	250	1.8	Mn ²⁺	250	7.5
Ba ²⁺	250	1.6	Cr ³⁺	12.5	-7.1
Mg ²⁺	250	1.1	SeO ₃ ²⁻	12.5	-5.4

Table 4S Effect of foreign substances on the determination of H₂O₂

Coexistent substance	Tolerance Concentratio n ($\mu\text{mol/L}$)	Relative error (%)	Coexistent substance	Tolerance Concentratio n ($\mu\text{mol/L}$)	Relative error (%)
K ⁺	1000	2.0	Mg ²⁺	1000	0.7
Ca ²⁺	500	-8.9	SeO ₃ ²⁻	2000	0.4
Zn ²⁺	1000	1.4	SO ₄ ²⁻	1000	2.8
Glucose	500	2.4	BrO ₃ ⁻	2500	3.6
BPO	250	6.1	Cu ²⁺	1000	3.1
Al ³⁺	250	-7.8	Mn ²⁺	75	8.6
Ba ²⁺	500	-8.7	Cr ³⁺	500	-7.6